Journal of Applied Mathematics and Physics, 2024, 12, 3384-3401
https://www.scirp.org/journal/jamp
ISSN Online: 2327-4379
ISSN Print: 2327-4352

Magnetohydrodynamic Conjugate Free Convective Heat Transfer Analysis of an Isothermal Horizontal Circular Cylinder with Temperature Dependent Viscosity

Nur Hosain Md. Ariful Azim

Department of Electrical and Electronic Engineering, Southeast University, Dhaka, Bangladesh
Email: nhmarif@seu.edu.bd

How to cite this paper: Azim, N.H.M.A. (2024) Magnetohydrodynamic Conjugate Free Convective Heat Transfer Analysis of an Isothermal Horizontal Circular Cylinder with Temperature Dependent Viscosity. *Journal of Applied Mathematics and Physics*, **12**, 3384-3401.
https://doi.org/10.4236/jamp.2024.1210201

Received: September 4, 2024
Accepted: October 14, 2024
Published: October 17, 2024

Abstract

Heat transfers due to MHD-conjugate free convection from the isothermal horizontal circular cylinder while viscosity is a function of temperature is investigated. The governing equations of the flow and connected boundary conditions are made dimensionless using a set of non-dimensional parameters. The governing equations are solved numerically using the finite difference method. Numerical results are obtained for various values of viscosity variation parameter, Prandtl number, magnetic parameter, and conjugate conduction parameter for the velocity and the temperature within the boundary layer as well as the skin friction coefficients and heat transfer rate along the surface.

Keywords

Conjugate Free Convection, Horizontal Circular Cylinder, Implicit Finite Difference Method, MHD, Temperature Dependent Viscosity

1. Introduction

Natural convective flow around heated, horizontal cylinders for various fluids is of great importance due to its extensive industrial applications. These applications have motivated extensive research on heat transfer and flow characteristics related to natural convection from horizontal cylinders [1]-[3]. The physical problem of heat transfer consists of the effect of conduction inside a solid body and convection on the surface of the solid, which is of significant importance in many real-life applications. The rate of heat transfer by conduction within a cylinder wall is influenced by the convection in the surrounding fluid. This type of heat transfer

process is known as conjugate heat transfer (CHT) problem. Considering its importance, many researchers have worked on it for various geometrical bodies [4]-[7]. Since the invention of magnetohydrodynamics (MHD), a lot of research has been accomplished to investigate the heat transfer behavior in the presence of MHD for various geometries [8]-[14].

All the above studies were confined to a fluid with constant viscosity. However, it is known that this physical property viscosity of the fluid may change significantly with temperature. In some heat-transfer problems, temperature differences are small compared with absolute temperature, and pressure differences are small compared with absolute pressure. Therefore, the changes in density, viscosity, and conductivity produced by the temperature differences are small enough to be neglected in the momentum and energy equation. However, in heat transfer problems with large temperature differences, the temperature-field equations become nonlinear and are coupled to the velocity-field equations, as the viscosity depends on the temperature. Viscosity may change significantly with temperature; for instance, the viscosity of water decreases by about 240% when the temperature increases from 10˚C (μ = 0.00131 kg·m^{-1}·s^{-1}) to 50˚C (μ = 0.000548 kg·m^{-1}·s^{-1}). To predict the flow behavior accurately, temperature dependent variation of viscosity is necessary to take into account. Gray *et al.* [15] and Mehta and Sood [16] showed that when the effect of variation of viscosity is considered, the flow characteristics may change substantially. Hossain *et al.* [17] studied the flow of viscous incompressible fluid with temperature-dependent viscosity and thermal conductivity (Proposed by Charraudeau ([18]) past a permeable wedge with variable heat flux. Elbashbeshy and Bazid [19] studied the effect of temperature-dependent viscosity on heat transfer over a continuously moving surface; they computed the velocity, temperature, skin friction and heat transfer rate for Prandtl number and viscosity parameter. Molla *et al.* [20] investigated effect of temperature dependent viscosity on natural convection flow from an isothermal horizontal circular cylinder and from a sphere. Ching-Yang Cheng [21] studied the effect of temperature-dependent viscosity on the natural convection heat transfer from a horizontal isothermal cylinder of elliptic cross section. Ahmad *et al.* [22] studied mixed convection boundary layer flow past an isothermal horizontal circular cylinder with temperature-dependent viscosity. The effect of temperature-dependent viscosity on the flow developed through a micro channel was studied by Kumar and Mahulikar [23]. They found four different flow regions and obtained the numerical results for those regions. Fluid flow considering temperature-dependent viscosity together with viscous dissipation past over a moving isothermal flat plate examined by Mutwiri *et al.* [24]. They found that increasing the viscosity variation parameter increases velocity and decreases temperature distribution. Hayat *et al.* [25] studied hydromagnetic peristalsis of water-based nanofluids with temperature-dependent viscosity. Miller *et al.* [26] studied the linear stability of the temperature-dependent boundary layer flow over a rotating disk. They show that the flow stability is affected highly by the change in the mean flow. Khan *et al.* [27] considered

temperature-dependent viscosity for bioconvection for non-Newtonian nanoparticles, they found that the increased viscosity parameter decreases velocity for non-newtonian nanoparticles. Quader and Alam [28] studied Soret and Dufour effects on unsteady free convection fluid flow in the presence of a hall current and heat flux. They have applied an explicit finite difference method to get solutions for heat transfer rate and fluid flow characteristics for various parameters such as heat source parameter, hall parameter, magnetic parameter, Eckert number, Dufour number and Soret number. Bouresli *et al.* [29] proposed a new model to predict the dynamic viscosity of a wide range of crude oils with various temperatures. Sangotayo *et al.* [30] investigated the heat characteristics and viscous flow in a moving isothermal cylindrical duct with Nanoparticles. Recently, Adekanmbi-Akinseye *et al.* [31] studied the Flow and Heat Transfer of a Dusty Williamson MHD Nanofluid Flow over a Permeable Cylinder in a Porous Medium. They presented the results graphically and discussed the effects of the parameters elaborately.

None of the above researchers considered magnetohydrodynamic (MHD) conjugate free convection flow from an isothermal horizontal circular cylinder with temperature-dependent viscosity. The present study will demonstrate this issue.

2. Physical Model

Consideration is given to a steady two-dimensional laminar free convective flow of a viscous, incompressible and electrically conducting fluid over a uniformly heated horizontal circular cylinder of radius *a*. It is assumed that the temperature of the surrounding fluid of the cylinder is T_∞. The cylinder has a heated core region of temperature T_b and the normal distance from inner surface to the outer surface is b with $T_b > T_\infty$.

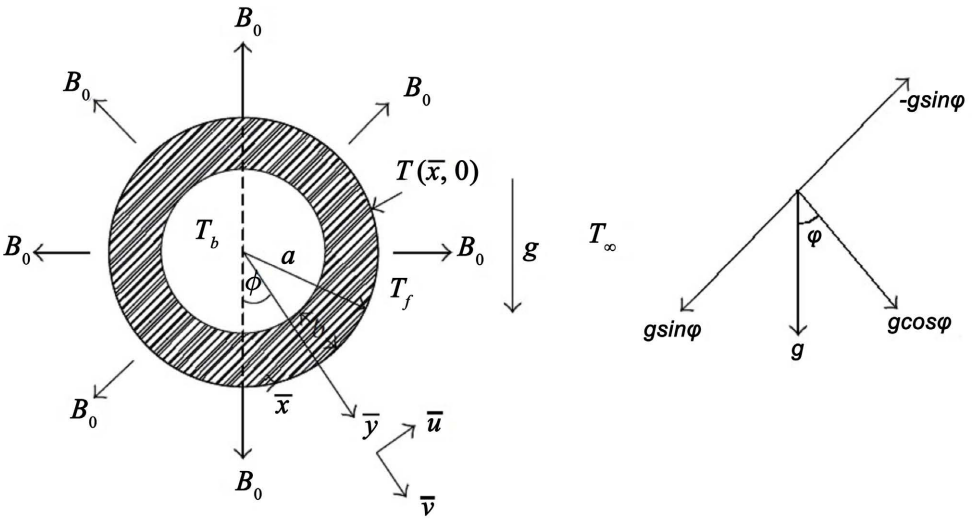

Figure 1. Physical model and coordinate system.

A uniform magnetic field having strength B_0 is acting normally on the cylinder surface. The physical model is shown in **Figure 1**, where the $\bar{x}$ -axis is taken

along the circumference of the cylinder measured from the lower stagnation point to the upper stagnation point and the $\bar{y}$ -axis is taken normal to the surface. The gravitational force g is acting in a downward direction.

3. Assumptions

The present research is based on the following assumptions:

1) The flow is steady, laminar, two-dimensional, incompressible, and electrically conducting.

2) The fluid may be treated as continuous and is describable in terms of local properties.

3) The cylinder surface is impermeable, with no injection or withdrawal at the wall.

4) The induced magnetic field is small enough to be negligible.

5) The Boussinesq approximation is applicable, which treats density as a constant in all terms in the governing equations except for the buoyancy term in the momentum equation. The density variation is mainly caused by the thermal expansion of the fluid and can be expressed as: $\rho(T)=\rho_{\infty}\left[1-\beta\left(T-T_{\infty}\right)\right]$ where $\beta=-\frac{1}{\rho}\left(\frac{\partial\rho}{\partial T}\right)_{p}$ denotes the coefficient of thermal expansion.

6) The boundary layer thickness is very small compared with the external radius "a" of the cylinder (Boundary layer approximation).

7) The viscosity of the fluid is a function of temperature, and other fluid properties are remained constant.

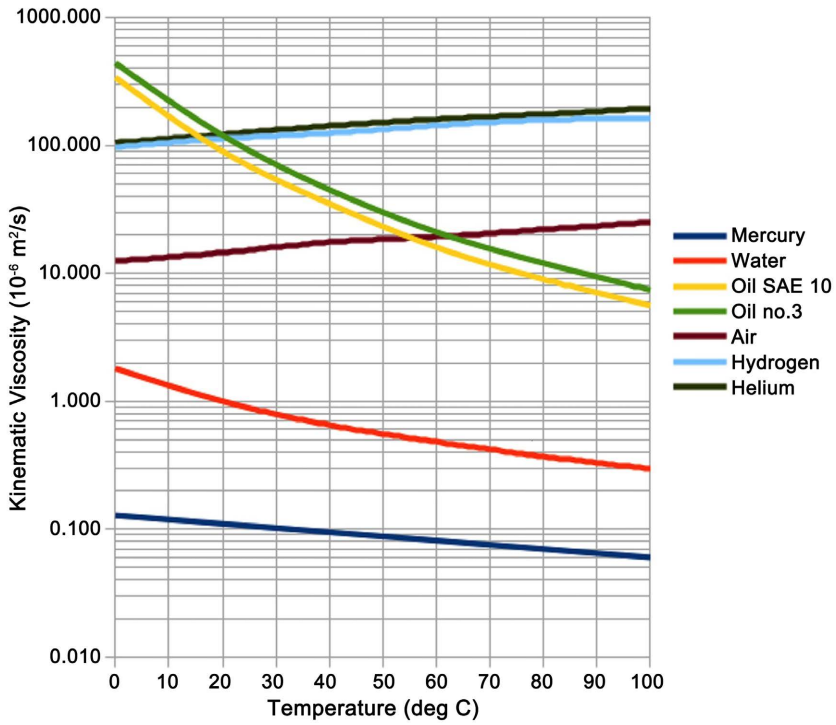

Figure 2. Variation of dynamic viscosity of several fluids with temperature.

Figure 2 shows the graphical presentation of dynamic viscosity for increasing the value of temperature. It is noted that the dynamic viscosity of some of the fluids, like engine oil, mercury, and water, etc., is inversely proportional to the linear function of temperature, whereas the viscosity of some of the fluids, like hydrogen and air are directly proportional to a linear function of temperature.

4. Governing Equations

Under the usual Boussinesq approximation, the equations governing this boundary-layer natural convection flow can be written as

$$\frac{\partial \overline{u}}{\partial \overline{x}}+\frac{\partial \overline{v}}{\partial \overline{y}}=0 \tag{1}$$

$$\overline{u}\frac{\partial \overline{u}}{\partial \overline{x}}+\overline{v}\frac{\partial \overline{u}}{\partial \overline{y}}=\frac{1}{\rho_\infty}\frac{\partial}{\partial \overline{y}}\left(\mu\frac{\partial \overline{u}}{\partial \overline{y}}\right)+g\beta_\infty\left(T_f-T_\infty\right)\sin\left(\frac{\overline{x}}{a}\right)-\frac{\sigma B_0^2\overline{u}}{\rho} \tag{2}$$

$$\overline{u}\frac{\partial T_f}{\partial \overline{x}}+\overline{v}\frac{\partial T_f}{\partial \overline{y}}=\frac{\kappa_f}{\rho_\infty\left(c_p\right)_\infty}\frac{\partial^2 T_f}{\partial \overline{y}^2} \tag{3}$$

The appropriate boundary conditions for the problem:

$$\begin{aligned}&\overline{u}=\overline{v}=0,\ T_f=T\left(\overline{x},0\right),\ \frac{\partial T_f}{\partial \overline{y}}=\frac{\kappa_s}{b\kappa_f}\left(T_f-T_b\right)\ \text{on}\ \overline{y}=0,\ x>0\\&\overline{u}\to 0,\ T_f\to T_\infty\ \text{as}\ \overline{y}\to\infty,\ \overline{x}>0\end{aligned} \tag{4}$$

Out of many forms of viscosity variation that are available in the literature, we have considered the following form proposed by Lings and Dybbs [32].

$$\mu=\frac{\mu_\infty}{1+\gamma\left(T_f-T_\infty\right)} \tag{5}$$

where γ is a constant and μ_∞ is the viscosity of the fluid outside the boundary layer.

$$\mu=\frac{\mu_\infty}{1+\gamma\left(\frac{T_f-T_\infty}{T_b-T_\infty}\right)T_b-T_\infty}=\frac{\mu_\infty}{1+\gamma\left(T_b-T_\infty\right)\theta}=\frac{\mu_\infty}{1+\lambda\theta} \tag{6}$$

where $\lambda=\gamma\left(T_b-T_\infty\right)$ is the viscosity variation parameter.

Grashof number $Gr=\left[g\beta a^3\left(T_b-T_\infty\right)\right]/\nu^2$, which is assumed large, and the following non-dimensional variables are used to make governing equations and boundary conditions dimensionless:

$$x=\frac{\overline{x}}{a},\ y=\frac{\overline{y}}{a}Gr^{1/4},\ u=\frac{\overline{u}a}{\nu}Gr^{-1/2},\ v=\frac{\overline{v}a}{\nu}Gr^{-1/4},\ \theta=\frac{T_f-T_\infty}{T_b-T_\infty} \tag{7}$$

where θ is the dimensionless temperature.

Using dimensionless variables described in Equation (7) and Equation (6), the first term of the right side of Equation (2) is

$$\frac{\partial}{\partial \overline{y}}\left(\mu\frac{\partial \overline{u}}{\partial \overline{y}}\right)=\frac{\partial}{\partial \overline{y}}\left(\frac{\mu_\infty}{1+\lambda\theta}\frac{\partial \overline{u}}{\partial \overline{y}}\right)=\mu_\infty\left(\frac{1}{1+\lambda\theta}\frac{\partial^2 \overline{u}}{\partial \overline{x}^2}+\frac{\partial \overline{u}}{\partial \overline{y}}\frac{\partial}{\partial \overline{y}}\left(1+\lambda\theta\right)^{-1}\right)$$

$$= \mu_\infty \left(\frac{1}{1+\lambda\theta} \frac{\nu_\infty Gr}{a^3} \frac{\partial^2 u}{\partial y^2} - \frac{\nu_\infty Gr^{\frac{1}{2}}}{a^2 Gr^{-\frac{1}{4}}} \frac{\partial u}{\partial y} \frac{1}{aGr^{-\frac{1}{4}}} (1+\lambda\theta)^{-2} \lambda \frac{\partial \theta}{\partial y} \right)$$

$$\therefore \frac{\partial}{\partial \bar{y}} \left(\mu \frac{\partial \bar{u}}{\partial \bar{y}} \right) = \mu_\infty \frac{\nu_\infty Gr}{a^3} \left(\frac{1}{1+\lambda\theta} \frac{\partial^2 u}{\partial y^2} - \frac{\lambda}{(1+\lambda\theta)^2} \frac{\partial u}{\partial y} \frac{\partial \theta}{\partial y} \right) \tag{8}$$

Applying Equations (7) and (8) in (2), a new form of the momentum equation is:

$$u\frac{\partial u}{\partial x} + v\frac{\partial u}{\partial y} + Mu = \frac{1}{1+\lambda\theta} \frac{\partial^2 u}{\partial y^2} - \frac{\lambda}{(1+\lambda\theta)^2} \frac{\partial u}{\partial y} \frac{\partial \theta}{\partial y} + \theta \sin x \tag{9}$$

where $M = \left(\sigma a^2 B_0^2\right) \Big/ \left(\nu_\infty \rho_\infty Gr^{1/2}\right)$ is the magnetic parameter and $\lambda = \gamma\left(T_b - T_\infty\right)$ is the temperature dependent viscosity variation parameter.

Applying (7) in (1), (3) and (4), the dimensionless form of the continuity equation, energy equation and the boundary conditions are:

$$\frac{\partial u}{\partial x} + \frac{\partial v}{\partial y} = 0 \tag{10}$$

$$u\frac{\partial \theta}{\partial x} + v\frac{\partial \theta}{\partial y} = \frac{1}{Pr} \frac{\partial^2 \theta}{\partial y^2} \tag{11}$$

$$\begin{aligned} &u = v = 0,\ \theta - 1 = \chi \frac{\partial \theta}{\partial y},\ \text{on } y = 0,\ x > 0 \\ &u \to 0,\ \theta \to 0 \text{ as } y \to \infty,\ x > 0 \end{aligned} \tag{12}$$

where, $Pr = \mu_\infty \left(c_p\right)_\infty \Big/ \kappa_f$ is the Prandtl number and $\chi = \left(b\kappa_f Gr^{1/4}\right) \Big/ \left(a\kappa_s\right)$ is the conjugate conduction parameter. Certainly, the present problem is governed by the magnetic parameter, viscosity variation parameter, Prandtl number, and conjugate conduction parameters. The present analysis will refer to the natural convection problem for $\chi = 0$.

To solve Equations (9), (10) and (11) subject to the boundary conditions in (12), we consider stream function and dimensionless temperature as:

$$\psi = x f\left(x, y\right),\quad \theta = \theta\left(x, y\right) \tag{13}$$

where θ is the dimensionless temperature and ψ is the stream function defined as:

$$u = \partial\psi / \partial y \quad \text{and} \quad v = -\partial\psi / \partial x \tag{14}$$

Substituting (13) and (14) into Equation (9) and (11), the new form of the dimensionless momentum and energy equations and the boundary conditions in (12) are:

$$\frac{1}{1+\lambda\theta} f''' + ff'' - f'^2 - \frac{\lambda}{(1+\lambda\theta)^2} \theta' f'' - Mf' + \frac{\sin x}{x}\theta = x\left(f' \frac{\partial f'}{\partial x} - f'' \frac{\partial f}{\partial x} \right) \tag{15}$$

$$\frac{1}{Pr}\theta'' + f\theta' = x\left(f' \frac{\partial \theta}{\partial x} - \theta' \frac{\partial f}{\partial x} \right) \tag{16}$$

$$\begin{aligned} &f = f' = 0,\ \theta - 1 = \chi \frac{\partial \theta}{\partial y} \text{ at } y = 0,\ x > 0 \\ &f' \to 0,\ \theta \to 0 \text{ as } y \to \infty,\ x > 0 \end{aligned} \tag{17}$$

The shearing stress in terms of skin friction coefficient is defined as

$$C_f = \frac{\tau_w}{\rho_\infty U_\infty^2} \tag{18}$$

where, U_∞ is the characteristic velocity and for free convection flows, defined as

$$U_\infty^2 = ga\beta\left(T_b - T_\infty\right) \tag{19}$$

The skin friction, by definition, is

$$\tau_w = \mu\left(\frac{\partial \bar{u}}{\partial \bar{y}}\right)_{\bar{y}=0} = \frac{\mu_\infty}{1+\lambda\theta}\frac{\nu_\infty Gr^{\frac{1}{2}}}{a^2 Gr^{-\frac{1}{4}}}\frac{\partial u}{\partial y} = \frac{\mu_\infty}{1+\lambda\theta}\frac{\nu_\infty Gr^{\frac{3}{4}}}{a^2} xf''(x,0) \tag{20}$$

Using the above relations in Equation (18), the skin friction coefficient is

$$C_f Gr^{\frac{1}{4}} = \frac{x}{1+\lambda\theta} f''(x,0) \tag{21}$$

The rate of heat transfer in terms of the Nusselt number can be determined by the equation

$$Nu = \frac{aq_w}{\kappa\left(T_w - T_\infty\right)} \tag{22}$$

$$\text{where,}\quad q_w = -\kappa\left(\frac{\partial T}{\partial \bar{y}}\right)_{\bar{y}=0} = -\kappa\frac{\left(T_w - T_\infty\right)Gr^{\frac{1}{4}}}{a}\theta'(x,0) \tag{23}$$

Using Equation (23) in Equation (22) gives the heat transfer coefficient as

$$Nu\, Gr^{-1/4} = -\theta(x,0) \tag{24}$$

The velocity profiles and temperature distributions within the boundary layer will be obtained from the equation

$$u = f'(x,y),\quad \theta = \theta(x,y) \tag{25}$$

Numerical results of the skin friction coefficient are determined from Equation (21), whereas the rate of heat transfer in terms of Nusselt number can be determined by Equation (24), and Equation (25) is accountable for the velocity profile and temperature distributions within the boundary layer.

5. Method of Solution

The implicit finite difference method has been employed to get the numerical solutions to the current problem, which was introduced by Keller [33] and elaborately describe by Cebeci and Bradshaw [34]. A brief discussion on the development of the algorithm of the implicit finite difference method, together with the Keller-box elimination scheme of the present analysis, is given below.

The Equations (15) and (16), based on the boundary conditions described in Equation (17), are written in terms of first-order equations in *y*, which are then expressed in finite difference form by approximating the functions and their derivatives in terms of the central differences in both coordinate directions. Denoting the mesh points in the (*x*, *y*) plane by x_i and y_j, where $i = 1,2,3,\cdots,M$

and $j = 1, 2, 3, \cdots, N$, central difference approximations are made such that the equations involving x explicitly are centred at $\left(x_{i-1/2}, y_{j-1/2}\right)$ and the remainder at $\left(x_i, y_{j-1/2}\right)$, where $y_{j-1/2} = \left(y_j + y_{j-1}\right)/2$, etc. This results in a set of nonlinear difference equations for the unknowns at x_i in terms of their values at x_{i-1}. These equations are then linearised by Newton's method and are solved using a block-tridiagonal algorithm, taking as the initial iteration of the converged solution at $x = x_{i-1}$. Now, to initiate the process at $x = 0$, we first provide guess profiles for all five variables (arising the reduction to the first order form) and use the Keller box method to solve the governing ordinary differential equations. Having obtained the lower stagnation point solution, it is possible to march step by step along the boundary layer. For a given value of x, the iterative procedure is stopped when the difference in computing the velocity and the temperature in the next iteration is less than 10^{-6}, *i.e.*, when $\left|\delta f^i\right| \le 10^{-6}$, where the superscript denotes the iteration number. The computations were not performed using a uniform grid in the y direction, but a non-uniform grid was used and defined by $y_j = \sinh\left(\left(j-1\right)/p\right)$, with $j = 1, 2, \cdots, 301$ and $p = 100$.

6. Results

There are four parameters in the governing equations that are very important to analyse the flow and heat transfer behaviour for the current problem. The two parameters in the momentum equation are magnetic parameter M and temperature-dependent viscosity variation parameter λ, one parameter in the energy equation, namely Prandtl number Pr, and one in the boundary condition, which is conjugate conduction parameter χ. The governing momentum Equation (15) and energy Equation (16) have been solved numerically based on the boundary condition (17) for different values of the above parameters using the implicit finite difference method together with the Keller box technique.

The Prandtl numbers are considered to be 3.50, 2.97, 1.63, and 1.00, corresponding to Dichlorodifluoromethane (Freon) at 50˚C, Methyl chloride at 50˚C, Glycerin at 50˚C and Steam at 700˚K respectively. The remaining parameters are taken as follows: magnetic parameter M = 0.0 - 0.5; conjugate conduction parameter χ = 0.0 - 2.0 and temperature-dependent viscosity variation parameter λ = 0.01 - 1.20.

Table 1 shows the comparison of the skin friction coefficient and local Nusselt number obtained in the present work with M = 0.0, χ = 0.0, λ = 0.0 and Pr = 1.0 and the results obtained by Merkin (1976) and Nazar *et al.* (2002). It has been observed that there is an excellent agreement among these results.

The maximum values of the velocities against y and maximum values of skin friction coefficients against x are shown in Tables 2-5 for different values of the viscosity variation parameter, magnetic parameter, Prandtl number and conjugate conduction parameter, respectively.

Figure 3, Figure 5, Figure 7 and Figure 9 illustrate the velocity and temperature distributions at $x = \pi/2$ against y, the direction along the normal to the surface

of the cylinder, and Figure 4, Figure 6, Figure 8 and Figure 10 depict the skin friction coefficients and heat transfer rates against x at $y = 0$ (along the surface of the cylinder) for different values of the viscosity variation parameter, magnetic parameter, Prandtl number and conjugate conduction parameter, respectively.

Table 1. Comparisons of the present numerical values of $xf''(x,0)$ and $-\theta'(x,0)$ with Merkin (1976) and Nazar *et al.* (2002) for different values of x while Prandtl number $Pr = 1.0$, magnetic parameter $M = 0.0$, conjugate conduction parameter $\chi = 0.0$ and temperature-dependent viscosity variation parameter $\lambda = 0.0$.

	$C_f Gr^{1/4} = xf''(x,0)$			$Nu\, Gr^{-1/4} = -\theta'(x,0)$		
x	Merkin (1976)	Nazar *et al.* (2002)	Present	Merkin (1976)	Nazar *et al.* (2002)	Present
0.0	0.0000	0.0000	0.000000	0.4214	0.4214	0.421414
π/6	0.4151	0.4148	0.414564	0.4161	0.4161	0.416130
π/3	0.7558	0.7542	0.753901	0.4007	0.4005	0.400500
π/2	0.9579	0.9545	0.954147	0.3745	0.3741	0.374069
2π/3	0.9756	0.9698	0.969669	0.3364	0.3355	0.335582
5π/6	0.7822	0.7740	0.773898	0.2825	0.2811	0.281234
π	0.3391	0.3265	0.326476	0.1945	0.1916	0.191783

Table 2. The maximum value of the velocities $f'(x,y)$ against y and the maximum value of the skin friction coefficient $xf''(x,0)$ against x for different values of temperature-dependent viscosity variation parameter λ while $Pr = 1.0$, $M = 0.1$ and $\chi = 1.0$.

Viscosity variation parameter λ	y	Maximum value of $f'(x,y)$	x	Maximum value of $xf''(x,0)$
0.01	1.438224	0.308463	1.884956	0.821498
0.40	1.302542	0.322075	1.884956	0.744191
0.80	1.237881	0.333891	1.884956	0.685632
1.20	1.114402	0.344185	1.884956	0.640179

Table 3. The maximum value of the velocities $f'(x,y)$ against y and the maximum value of the skin friction coefficient $xf''(x,0)$ against x for different values of magnetic parameter M with $Pr = 1.0$, $\chi = 1.0$, and $\lambda = 0.01$.

Magnetic parameter M	y	Maximum value of $f'(x,y)$	x	Maximum value of $xf''(x,0)$
0.0	1.438224	0.317195	1.919862	0.839187
0.1	1.438224	0.308463	1.884956	0.821498
0.3	1.438224	0.292272	1.850049	0.788942
0.5	1.438224	0.277603	1.850049	0.759936

Table 4. The maximum value of the velocities $f'(x,y)$ against y and the maximum value of the skin friction coefficient $xf''(x,0)$ against x for different values of magnetic parameter M with $Pr = 1.0$, $\chi = 1.0$, and $\lambda = 0.01$.

Prandtl number Pr	y	Maximum value of $f'(x,y)$	x	Maximum value of $xf''(x,0)$
1.00	1.438224	0.308463	1.884956	0.821498
1.63	1.369287	0.260281	1.884956	0.733352
2.97	1.302542	0.207878	1.884956	0.631341
3.50	1.302542	0.194862	1.884956	0.604892

Table 5. The maximum value of the velocities $f'(x,y)$ against y and the maximum value of the skin friction coefficient $xf''(x,0)$ against x for different values of magnetic parameter M with $Pr = 1.0$, $\chi = 1.0$, and $\lambda = 0.01$.

Conjugate conduction parameter χ	y	Maximum value of $f'(x,y)$	x	Maximum value of $xf''(x,0)$
0.0	1.369287	0.346776	1.850049	0.963528
1.0	1.438224	0.324516	1.884956	0.880927
1.5	1.438224	0.308463	1.884956	0.821498
2.0	1.509461	0.286700	1.884956	0.741197

The effects of the temperature-dependent viscosity variation parameter λ on the velocity and temperature distribution are illustrated in **Figure 3(a)** and **Figure 3(b),** respectively, while Prandtl number $Pr = 1.0$, magnetic parameter $M = 0.1$ and conjugate conduction parameter $\chi = 1.0$. Then again, **Figure 4(a)** and **Figure 4(b)** show the influence of the temperature-dependent viscosity variation parameter λ on the skin friction coefficient and the rate of heat transfer, respectively. It has been observed from Equation (6) that the viscosity of the fluid within the boundary layer decreases with increasing value of viscosity variation parameter λ. As the viscosity of the fluid within the boundary layer decreases with increasing viscosity variation parameters, accordingly the velocity increases and the skin friction coefficient decreases with increasing viscosity variation parameters, as observed in **Figure 3(a)** and **Figure 4(a)** respectively. From **Figure 3(b)**, it is seen that the temperature within the boundary layer slightly decreases with increasing value of the viscosity variation parameter λ, which leads to an increase in heat transfer rate as found in **Figure 4(b)**. Moreover, it is found from **Figure 3(a)** and from **Table 2** that the maximum velocity becomes closer to the surface as we consider the higher value of viscosity variation parameter λ. The maximum values of the velocities are reported as 0.308463, 0.322075, 0.333891 and 0.344185 at $y =$ 1.438224, 1.302542, 1.237881 and 1.114402 for viscosity variation parameter $\lambda =$ 0.01, 0.40, 0.80 and 1.20 respectively. Alternatively, it is also reported that the maximum values of the skin friction coefficient are 0.821498, 0.744191, 0.685632 and

0.640179 at $x = 1.884956$ for viscosity variation parameter $\lambda = 0.01$, 0.40, 0.80 and 1.20 respectively. Therefore, it is concluded that the maximum velocity increases by 11.58%, and the maximum value of the skin friction coefficient decreases by 22.07% as the viscosity variation parameter λ increases from 0.01 to 1.20.

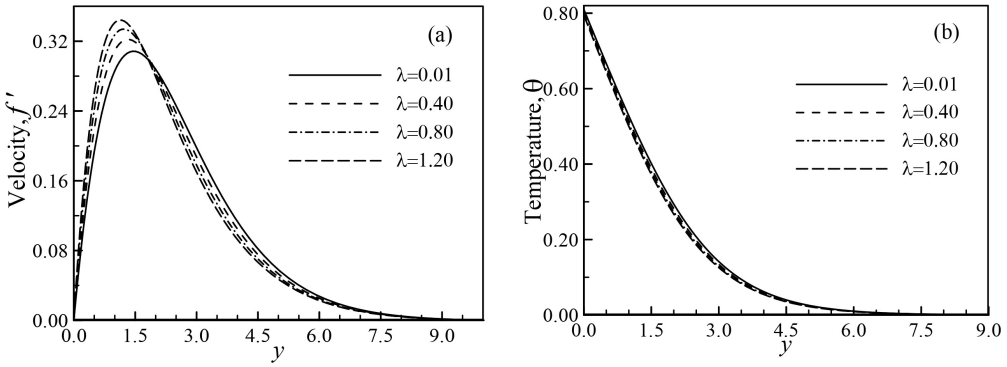

Figure 3. (a) Variation of velocity profiles and (b) variation of temperature profiles against y for varying of viscosity variation parameter λ with $Pr = 1.0$, $M = 0.1$, $\chi = 1.0$ and $\lambda = 0.01$.

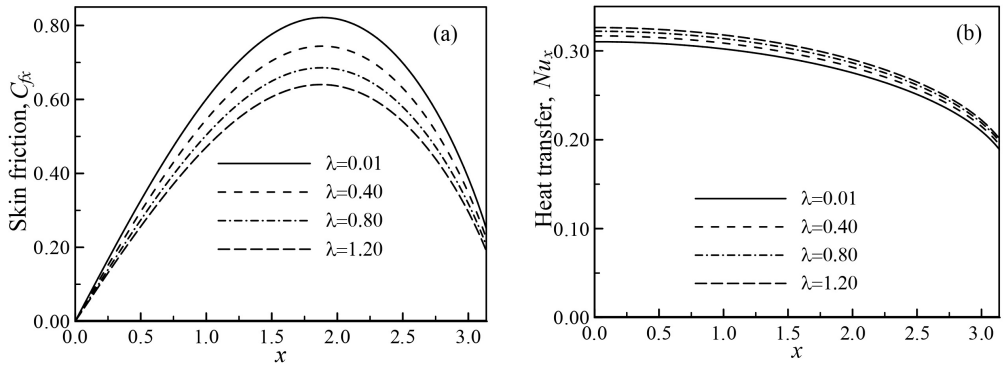

Figure 4. (a) Variation of the local skin friction coefficients and (b) variation of local Nusselt number against x for varying of viscosity variation parameter λ with $Pr = 1.0$, $M = 0.1$, $\chi = 1.0$ and $\lambda = 0.01$.

It is observed from Figure 5(a) that the motion of the fluid decreases within the boundary layer for increasing value of the magnetic parameter M, if temperature-dependent viscosity is taken into account. Therefore, the skin friction coefficient at the surface of the cylinder is decreased, which is shown in Figure 6(a). The temperature within the thermal boundary layer increases with increasing value of the magnetic parameters, as revealed in Figure 5(b), and the heat transfer rate decreases with increasing magnetic parameters, as illustrated in Figure 6(b). The maximum values of the velocity are recorded to be 0.317195, 0.308463, 0.292272 and 0.277603, and the maximum values of the skin friction coefficient are 0.839187, 0.821498, 0.788942 and 0.759936 for magnetic parameter $M = 0.0$, 0.1, 0.3 and 0.5 respectively with viscosity variation parameter $\lambda = 0.01$, which are presented in Table 3. Here, it is observed that the velocity decreases by 12.48% and the skin friction coefficient decreases by 9.44% when the value of the magnetic parameter changes from 0.0 to 0.5 in the presence of the viscosity variation parameter.

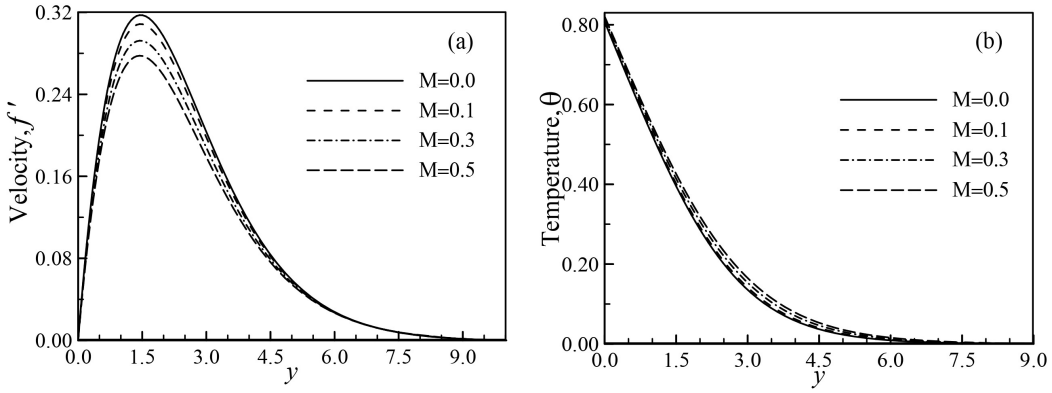

Figure 5. (a) Variation of velocity profiles and (b) variation of temperature profiles against y for varying magnetic parameter M with $Pr = 1.0$, $\chi = 1.0$ and $\lambda = 0.01$.

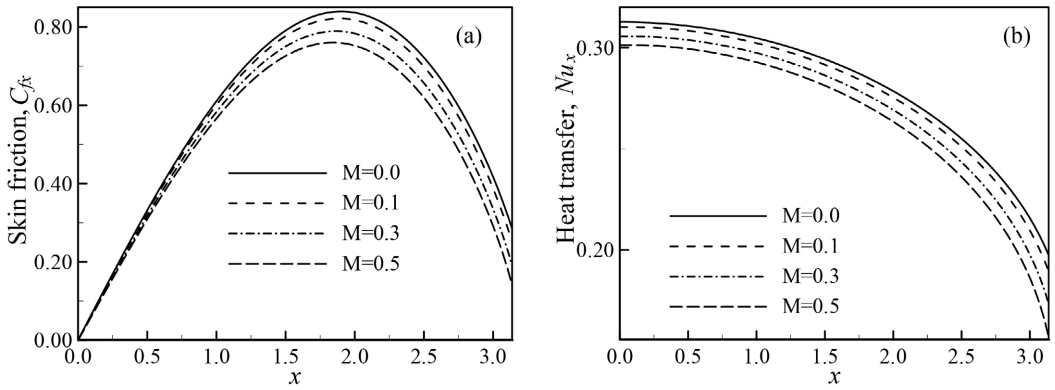

Figure 6. (a) Variation of the local skin friction coefficients and (b) variation of local Nusselt number against x for varying magnetic parameter M with $Pr = 1.0$, $\chi = 1.0$ and $\lambda = 0.01$.

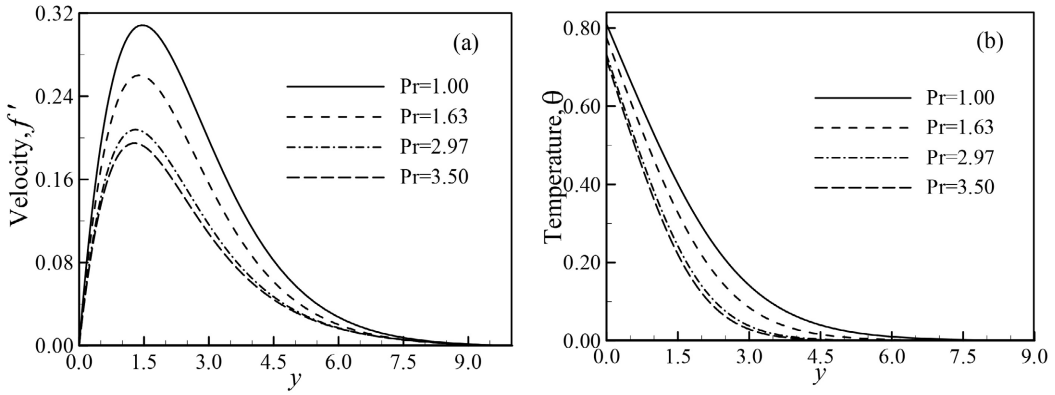

Figure 7. (a) Variation of velocity profiles and (b) variation of temperature profiles against y for varying of Prandtl number Pr with $M = 0.1$, $\chi = 1.0$ and $\lambda = 0.01$.

The velocity profiles and temperature profiles are plotted against the y-axis in Figure 7, and the skin friction coefficient and heat transfer rate are plotted against the x-axis in Figure 8 for different values of Prandtl number with $M = 0.1$, $\chi = 1.0$ and $\lambda = 0.01$. The velocity and temperature of fluid are expected to decrease with the increasing Prandtl number, which is observed in Figure 7(a) and Figure 7(b)

respectively. Thus, the skin friction decreases and the heat transfer rate from the core region to the boundary layer region increases for increasing value of Prandtl number as depicted in Figure 8(a) and Figure 8(b), respectively. Table 4 shows the maximum values of the velocities and the maximum values of the skin friction coefficients, respectively, for different values of Prandtl numbers. It has been observed that the maximum values of the velocities are 0.308463, 0.260281, 0.207878 and 0.194862, whereas the maximum values of the skin friction coefficient are 0.821498, 0.733352, 0.631341and 0.604892 for Prandtl numbers Pr = 1.00, 1.63, 2.97 and 3.50 respectively. It is noted that the velocity and the skin friction coefficient decrease by 36.83% and 26.37%, respectively, as the Prandtl number changes from 1.0 to 3.5.

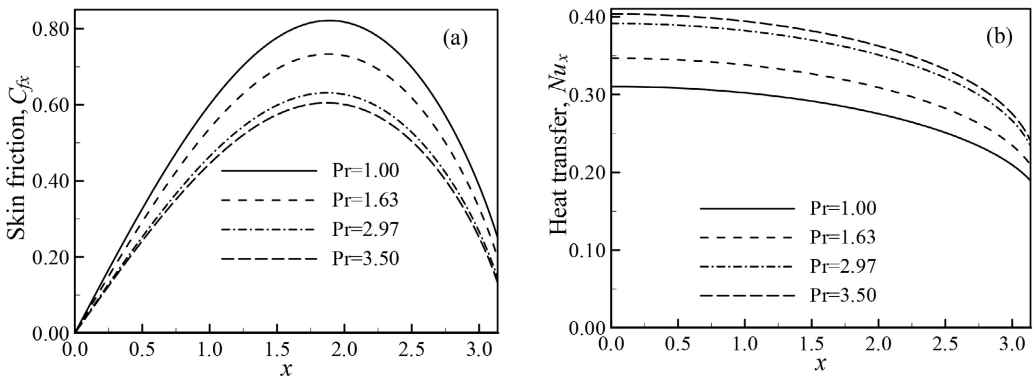

Figure 8. (a) Variation of the local skin friction coefficients and (b) variation of local Nusselt number against x varying of Prandtl number Pr with M = 0.1, χ = 1.0 and λ = 0.01.

Figure 9(a) and Figure 9(b) illustrate the effects of the conjugate conduction parameter χ on the fluid velocity and temperature distributions, respectively. On the other hand, Figure 10(a) and Figure 10(b) depict the variation of the conjugate conduction parameter χ on the skin friction coefficient and the heat transfer rate with Pr = 1.0, M = 0.1 and λ = 0.01. From the definition of the conjugate conduction parameter, we found that the increasing value of the conjugate conduction parameter χ is a result of the high thickness of the cylinder and the low conductivity of the element of the cylinder. So, it obviously resists conduction from the core region to the boundary layer and, consequently, decelerates convection within the boundary layer. As a result, velocity and temperature decrease for increasing values of the conjugate conduction parameters at a particular value of y, which are presented in Figure 9(a) and Figure 9(b), respectively. As the velocity decreases, the skin friction at the surface decreases for increasing value of conjugate conduction parameter χ, as observed in Figure 10(a). Since increasing the value of the conjugate conduction parameters resists conduction from the core region to the boundary layer, as mentioned earlier, it, of course, resists heat transfer, which is observed in Figure 10(b). It is observed the local Nusselt number and the skin friction coefficient both decrease with increasing value of the conjugate conduction parameter χ. The maximum values of the velocity and the skin friction

coefficient are presented in Table 5. It can be noted that the maximum values of the velocity are 0.346776, 0.324516, 0.308463 and 0.286700 at y = 1.369287, 1.438224, 1.438224 and 1.509461 and the maximum values of the skin friction coefficient are 0.963528, 0.880927, 0.821498 and 0.741197 for conjugate conduction parameter χ = 0.0, 1.0, 1.5 and 2.0 respectively. At the end of this section, it is found that the velocity and the skin friction coefficient decreased by 17.32% and 23.07%, respectively, as the conjugate conduction parameter changes from 0.0 to 2.0.

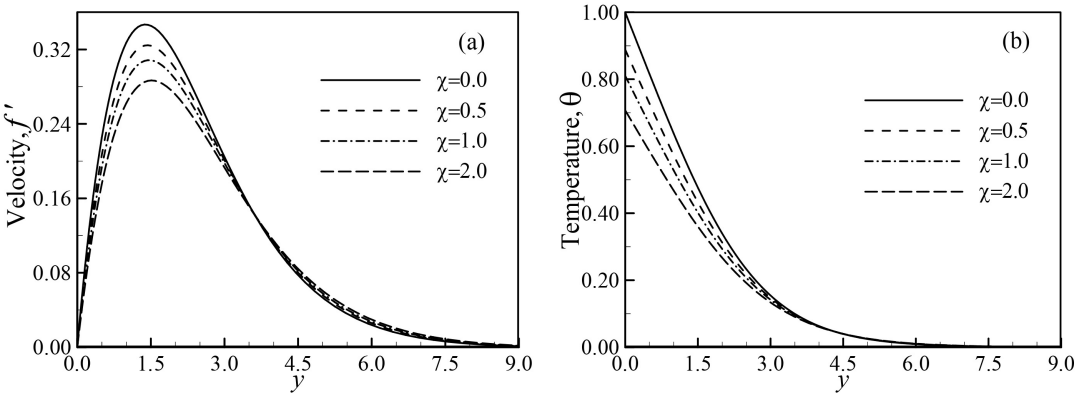

Figure 9. (a) Variation of velocity profiles and (b) variation of temperature profiles against y for varying of conjugate conduction parameter χ with Pr = 1.0, M = 0.1 and λ = 0.01.

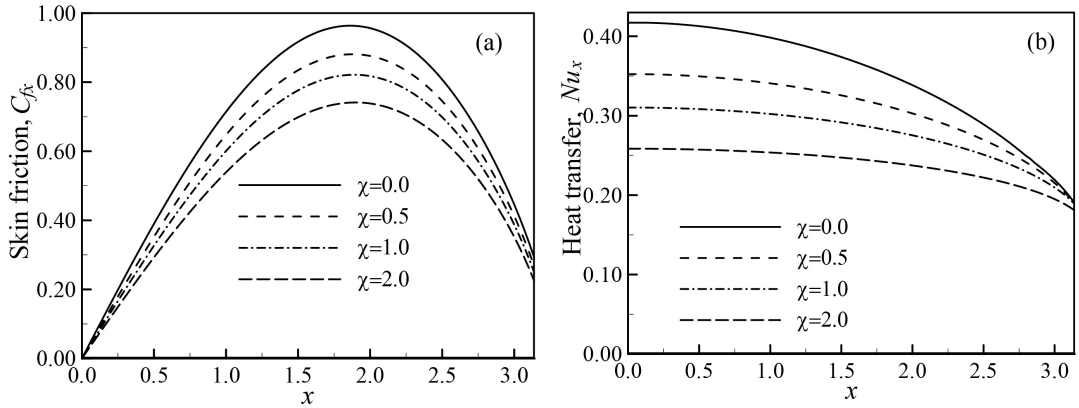

Figure 10. (a) Variation of the local skin friction coefficients and (b) variation of local Nusselt number against x for varying of conjugate conduction parameter χ with Pr = 1.0, M = 0.1 and λ = 0.01.

7. Conclusion

The effect of temperature-dependent viscosity on MHD-conjugate free convection flow from an isothermal horizontal circular cylinder is studied. The flow and heat transfer are governed by the viscosity variation parameter, Magnetic parameter, Prandtl number, and conjugate conduction parameter. It is found that the velocity increases and the temperature decreases within the boundary layer for increasing values of the viscosity variation parameter, while as the skin friction decreases and heat transfer increases with increasing viscosity variation parameter.

In the presence of temperature-dependent viscosity, the velocity and the skin friction decrease with increasing values of the magnetic parameter, Prandtl number and conjugate conduction parameter; temperature increases for increasing value of magnetic parameter whereas it decreases for increasing Prandtl number and conjugate conduction parameter. Heat transfer rate decreases for increasing magnetic parameter and conjugate conduction parameter; however, it increases for increasing value of Prandtl number. The study also opens a platform for a number of research works, such as considering the effects of joule heating, heat generation, stress work, viscous dissipation, temperature-dependent thermal conductivity, etc.

Conflicts of Interest

The author declares no conflicts of interest regarding the publication of this paper.

References

[1] Merkin, J.H. (1976) Free Convection Boundary Layer on an isothermal a Clinic Cylinder. *Journal of Applied Mathematics and Physics*, **29**, 871-883.

[2] Kuehn, T.H. and Goldstein, R.J. (1980) Numerical Solution to the Navier-Stokes Equations for Laminar Natural Convection about a Horizontal Isothermal Circular Cylinder. *International Journal of Heat and Mass Transfer*, **23**, 971-979. https://doi.org/10.1016/0017-9310(80)90071-x

[3] Wang, P., Kahawita, R. and Nguyen, T.H. (1990) Numerical Computation of the Natural Convection Flow about a Horizontal Cylinder Using Splines. *Numerical Heat Transfer*, *Part A*: *Applications*, **17**, 191-215. https://doi.org/10.1080/10407789008944739

[4] Gdalevich, L.B. and Fertman, V.E. (1977) Conjugate Problems of Natural Convection. *Journal of Engineering Physics*, **33**, 1120-1126. https://doi.org/10.1007/bf00860563

[5] Miyamoto, M., Sumikawa, J., Akiyoshi, T. and Nakamura, T. (1980) Effects of Axial Heat Conduction in a Vertical Flat Plate on Free Convection Heat Transfer. *International Journal of Heat and Mass Transfer*, **23**, 1545-1553. https://doi.org/10.1016/0017-9310(80)90158-1

[6] Pozzi, A. and Lupo, M. (1988) The Coupling of Conduction with Laminar Natural Convection along a Flat Plate. *International Journal of Heat and Mass Transfer*, **31**, 1807-1814. https://doi.org/10.1016/0017-9310(88)90195-0

[7] Kimura, S. and Pop, I. (1994) Conjugate Natural Convection from a Horizontal Circular Cylinder. *Numerical Heat Transfer*, *Part A*: *Applications*, **25**, 347-361. https://doi.org/10.1080/10407789408955953

[8] Wilks, G. (1976) Magnetohydrodynamic Free Convection about a Semi-Infinite Vertical Plate in a Strong Cross Field. *Zeitschrift für angewandte Mathematik und Physik*, **27**, 621-631. https://doi.org/10.1007/bf01591174

[9] Takhar, H.S. and Soundalgekar, V.M. (1980) Dissipation Effects on MHD Free Convection Flow Past a Semi-Infinite Vertical Plate. *Applied Scientific Research*, **36**, 163-171. https://doi.org/10.1007/bf00386469

[10] Hossain, M.A. (1992) Viscous and Joule Heating Effects on Mhd-Free Convection Flow with Variable Plate Temperature. *International Journal of Heat and Mass Transfer*, **35**, 3485-3487. https://doi.org/10.1016/0017-9310(92)90234-j

[11] Aldoss, T.K., Ali, Y.D. and Al-Nimr, M.A. (1996) Mhd Mixed Convection from a Horizontal Circular Cylinder. *Numerical Heat Transfer*, *Part A*: *Applications*, **30**, 379-396. https://doi.org/10.1080/10407789608913846

[12] Yih, K.A. (1999) MHD Forced Convection Flow Adjacent to a Non-Isothermal Wedge. *International Communications in Heat and Mass Transfer*, **26**, 819-827. https://doi.org/10.1016/s0735-1933(99)00070-6

[13] El-Amin, M.F. (2003) Combined Effect of Viscous Dissipation and Joule Heating on MHD Forced Convection over a Non-Isothermal Horizontal Cylinder Embedded in a Fluid Saturated Porous Medium. *Journal of Magnetism and Magnetic Materials*, **263**, 337-343. https://doi.org/10.1016/s0304-8853(03)00109-4

[14] Molla, M.M., Hossain, M.A. and Paul, M.C. (2006) Natural Convection Flow from an Isothermal Horizontal Circular Cylinder in Presence of Heat Generation. *International Journal of Engineering Science*, **44**, 949-958. https://doi.org/10.1016/j.ijengsci.2006.05.002

[15] Gary, J., Kassoy, D.R., Tadjeran, H. and Zebib, A. (1982) The Effects of Significant Viscosity Variation on Convective Heat Transport in Water-Saturated Porous Media. *Journal of Fluid Mechanics*, **117**, 233-249. https://doi.org/10.1017/s0022112082001608

[16] Mehta, K.N. and Sood, S. (1992) Transient Free Convection Flow with Temperature Dependent Viscosity in a Fluid Saturated Porous Medium. *International Journal of Engineering Science*, **30**, 1083-1087. https://doi.org/10.1016/0020-7225(92)90032-c

[17] Hossain, M.A., Munir, M.S. and Rees, D.A.S. (2000) Flow of Viscous Incompressible Fluid with Temperature Dependent Viscosity and Thermal Conductivity Past a Permeable Wedge with Uniform Surface Heat Flux. *International Journal of Thermal Sciences*, **39**, 635-644. https://doi.org/10.1016/s1290-0729(00)00227-1

[18] Charraudeau, J. (1975) Influence de gradients de proprietes physiques en convection forcee—Application au cas du tube. *International Journal of Heat and Mass Transfer*, **18**, 87-95. https://doi.org/10.1016/0017-9310(75)90011-3

[19] Elbashbeshy, E.M.A. and Bazid, M.A.A. (2000) The Effect of Temperature-Dependent Viscosity on Heat Transfer over a Continuous Moving Surface. *Journal of Physics D*: *Applied Physics*, **33**, 2716-2721. https://doi.org/10.1088/0022-3727/33/21/309

[20] Molla, M.M., Hossain, M.A. and Gorla, R.S.R. (2001) Natural Convection Flow from an Isothermal Horizontal Circular Cylinder with Temperature Dependent Viscosity. *Heat Mass Transfer*, *Part A*, **44**, 827-836.

[21] Cheng, C. (2006) The Effect of Temperature-Dependent Viscosity on the Natural Convection Heat Transfer from a Horizontal Isothermal Cylinder of Elliptic Cross Section. *International Communications in Heat and Mass Transfer*, **33**, 1021-1028. https://doi.org/10.1016/j.icheatmasstransfer.2006.02.019

[22] Ahmad, S., Arifin, N.M., Nazar, R. and Pop, I. (2009) Mixed Convection Boundary Layer Flow Past an Isothermal Horizontal Circular Cylinder with Temperature-Dependent Viscosity. *International Journal of Thermal Sciences*, **48**, 1943-1948. https://doi.org/10.1016/j.ijthermalsci.2009.02.014

[23] Kumar, R. and Mahulikar, S.P. (2015) Effect of Temperature-Dependent Viscosity Variation on Fully Developed Laminar Microconvective Flow. *International Journal of Thermal Sciences*, **98**, 179-191. https://doi.org/10.1016/j.ijthermalsci.2015.07.011

[24] Mutwiri, E., Mwenda, E. and Karanja, S. (2016) Effects of Temperature Dependent Viscosity and Viscous Dissipation on Fluid Flow Past a Moving Isothermal Flat Plate. *International Journal of Innovative Science*, *Engineering & Technology*, **3**, 131-142.

[25] Hayat, T., Ahmed, B., Abbasi, F.M. and Alsaedi, A. (2017) Hydromagnetic Peristalsis of Water Based Nanofluids with Temperature Dependent Viscosity: A Comparative Study. *Journal of Molecular Liquids*, **234**, 324-329. https://doi.org/10.1016/j.molliq.2017.03.080

[26] Miller, R., Griffiths, P.T., Hussain, Z. and Garrett, S.J. (2020) On the Stability of a Heated Rotating-Disk Boundary Layer in a Temperature-Dependent Viscosity Fluid. *Physics of Fluids*, **32**, Article 024105. https://doi.org/10.1063/1.5129220

[27] Khan, M.I., Khan, S.U., Jameel, M., Chu, Y., Tlili, I. and Kadry, S. (2021) Significance of Temperature-Dependent Viscosity and Thermal Conductivity of Walter's B Nanoliquid When Sinusodal Wall and Motile Microorganisms Density Are Significant. *Surfaces and Interfaces*, **22**, Article 100849. https://doi.org/10.1016/j.surfin.2020.100849

[28] Quader, A. and Alam, M.M. (2021) Soret and Dufour Effects on Unsteady Free Convection Fluid Flow in the Presence of Hall Current and Heat Flux. *Journal of Applied Mathematics and Physics*, **9**, 1611-1638. https://doi.org/10.4236/jamp.2021.97109

[29] Bouresli, K., Ma, X., Albazzaz, H. and Jose, S. (2023) Development of a New Temperature-Dependent Viscosity Model for Crude Oils. *Industrial & Engineering Chemistry Research*, **62**, 11186-11193. https://doi.org/10.1021/acs.iecr.3c01213

[30] Sangotayo, E.O., Adedeji, K.A. and Ogidiga, J.O. (2023) Heat Characteristics and Viscous Flow in a Moving Isothermal Cylindrical Duct with Nanoparticles. *Journal of Applied Mathematics and Physics*, **11**, 2361-2372. https://doi.org/10.4236/jamp.2023.118151

[31] Adekanmbi-Akinseye, O.A., Fenuga, O.J., Isede, H.A. and Sobamowo, M.G. (2024) Flow and Heat Transfer of a Dusty Williamson MHD Nanofluid Flow over a Permeable Cylinder in a Porous Medium. *Open Journal of Fluid Dynamics*, **14**, 100-122. https://doi.org/10.4236/ojfd.2024.142005

[32] Ling, J.X. and Dybbs, A. (1987) Forced Convection over a Flat Plate Submersed in a Porous Medium: Variable Viscosity Case. Paper 87-WA/HT-23. American Society of Mechanical Engineers.

[33] Keller, H.B. (1978) Numerical Methods in Boundary-Layer Theory. *Annual Review of Fluid Mechanics*, **10**, 417-433. https://doi.org/10.1146/annurev.fl.10.010178.002221

[34] Cebeci, T. and Bradshaw, P. (1984) Physical and Computational Aspects of Convective Heat Transfer. Springer.

Nomenclature

Symbol	Meaning
a	Radius of the cylinder
b	Thickness of the cylinder
B_0	Applied magnetic field
C_{fx}	Skin friction coefficient
c_p	Specific heat
f	Dimensionless stream function
g	Acceleration due to gravity
M	Magnetic parameter
Nu_x	Local Nusselt number
Pr	Prandtl number
T_b	Temperature of the inner cylinder
T_f	Temperature at the boundary layer region
T_s	Temperature of the solid of the cylinder
T_∞	Temperature of the ambient fluid
$\overline{u}, \overline{v}$	Velocity components
u, v	Dimensionless velocity components
$\overline{x}, \overline{y}$	Cartesian coordinates
x, y	Dimensionless Cartesian coordinates
Greek symbol	Meaning
β	Co-efficient of thermal expansion
χ	Conjugate conduction parameter
ψ	Dimensionless stream function
λ	Viscosity variation parameter
ρ	Density of the fluid inside the boundary layer
ν	Kinematic viscosity
μ	Viscosity of the fluid
θ	Dimensionless temperature
σ	Electrical conductivity
κ_f	Thermal conductivity of the ambient fluid
κ_s	Thermal conductivity of the ambient solid